Bulk-limited electrical behaviors in metal/hydrogenated diamond-like carbon/metal devices

Peng Guo, Rende Chen, Lili Sun, Xiaowei Li, Peiling Ke, Qunji Xue, and Aiying Wang

Bulk-limited electrical behaviors in metal/hydrogenated diamond-like carbon/metal devices

Peng Guo,[1] Rende Chen,[1] Lili Sun,[1] Xiaowei Li,[1,2] Peiling Ke,[1] Qunji Xue,[1] and Aiying Wang[1,a)]

[1]*Key Laboratory of Marine Materials and Related Technologies, Zhejiang Key Laboratory of Marine Materials and Protective Technologies, Ningbo Institute of Materials Technology and Engineering, Chinese Academy of Sciences, 315201 Ningbo, People's Republic of China*
[2]*Computational Science Center, Korea Institute of Science and Technology, Seoul 136-791, South Korea*

Regardless of used metal contact combinations, bulk-limited electrical behaviors were observed in metal/hydrogenated diamond-like carbon (DLC)/metal (MSM) devices through the study of I-V curves and temperature dependence of conductivity. For MSM devices with DLC deposited at a substrate bias of -50 V, the I-V curves exhibited ohmic electrical behaviors in the range of 0–1 V and followed the Poole-Frenkel mechanism in the range of 1–5 V. Moreover, the carrier transport was dominated by the thermally activated process with an activation energy of 0.1576 eV in the temperature range of 160–400 K. The bulk-limited behaviors of MSM devices could be attributed to the relatively high bulk resistance of the DLC layer. This result offers the fundamental insight into DLC based electrical devices and brings forward the concept to fabricate functional carbon based materials. *Published by AIP Publishing.* https://doi.org/10.1063/1.5003297

As amorphous semiconductor materials, diamond-like carbon (DLC) films have attracted much attention, since their optical gap can range from 1 to 4 eV and their electrical resistivity can span 14 orders of magnitude by adjusting the sp^2/sp^3 ratio in the carbon matrix.[1,2] Nowadays, many efforts have been dedicated to explore their novel functional and electrical applications, such as piezoresistive sensors,[3] solar cells,[4] and potential memory devices.[5,6] Usually, the metal/semiconductor (DLC)/metal (MSM) structure would be fabricated for the cells or modules, which will significantly dominate the performance of electrical devices.[7–12] Unfortunately, due to the feature diversity of the DLC films deposited by different processing and the complexity of the interfacial interaction between metal and C elements, various mechanisms involving DLC/metal interface-limited and bulk-limited electrical behaviors were achieved for such MSM structured devices. Allon-Alaluf *et al.*[8] reported that the DLC/metal interface-limited electrical behaviors originated from the formation of an interface barrier, when Al was used as upper and bottom contacts, which was conflicted with the bulk-limited electrical behaviors with the Al or Cr upper contact reported by Egret and co-workers.[13] In addition, Paul and Clough[12] found that for the MSM structure with the Cr bottom contact, both interface-limited and bulk-limited electrical behaviors appeared, depending on the area of the upper metal (Al, W, Ni, and Au) contacts. Since the electrical behavior of structured MSM plays a key role in the whole performance of carbon-based devices, the contradictory of electrical experimental results makes it important to reveal the inherent carrier transport mechanism of the DLC MSM devices.

In this work, hydrogenated DLC films were prepared by a linear ion source (LIS)[14] at various bias voltages of -50 V, -100 V, -150 V, and -200 V. C_2H_2 gas with a flow rate of 38 sccm was introduced to the LIS to obtain the hydrogenated carbon ions, and the working pressure was kept at 2.6×10^{-3} Pa. The power for LIS was about 260 W, with a DC of 0.2 A and a voltage of 1100–1450 V (more details can be found in the supplementary material). A series of MSM devices with 4 different metal contact combinations were fabricated. Two common metal elements were selected as contacts for comparison. Namely, one is Al, a typical weak-carbide-forming metal and inclined to form an interface barrier.[8] The other one is Cr, a typical strong-carbide-forming metal and inclined to form conductive carbides.[13] The MSM structures [as shown in Fig. 1(a)] were fabricated as follows. First, the metal (Al 80 nm/Cr 390 nm) bottom contact film was sputtered onto the p-type silicon wafer (100), and then, DLC films with a thickness of 470 ± 50 nm were deposited at room temperature (RT). Finally, the upper metal (Al 280 nm/Cr 200 nm) contact dots (with a diameter of approximately 200 μm and a contact area of 3.1×10^{-8} m^2) were fabricated with the same sputtering system through a shadow mask. Raman spectroscopy (Renishaw inVia-reflex, 532 nm) was used to measure the carbon atomic bonds from 800 to 2000 cm^{-1} wavenumber. A field-emission transmission electron microscope (TEM, Libra 200 FE, Zeiss, Germany) at an operating voltage of 200 kV was used to investigate the film morphology. A Lakeshore probe station equipped with a precision semiconductor parameter analyzer (Keithley 4200) in the DC sweep mode was applied to measure the current-voltage (I-V) characteristics of the MSM devices. Here, symbol D_{asy} was used to evaluate the I-V asymmetry, which was defined as the absolute value of the ratio of I_n to I_p, which was $D_{asy} = |I_n/I_p|$, where I_n and I_p are the negative current and positive current at the corresponding negative and positive applied voltages, respectively. We focused the temperature dependence of dark electrical conductivity (σ) of the DLC in the range of 160–400 K. Before the measurement of σ, all samples were heated to 400 K to minimize the possible

a)Author to whom correspondence should be addressed: aywang@nimte.ac.cn. Tel.: +86-574-86685170.

(a)

(b)

(c)
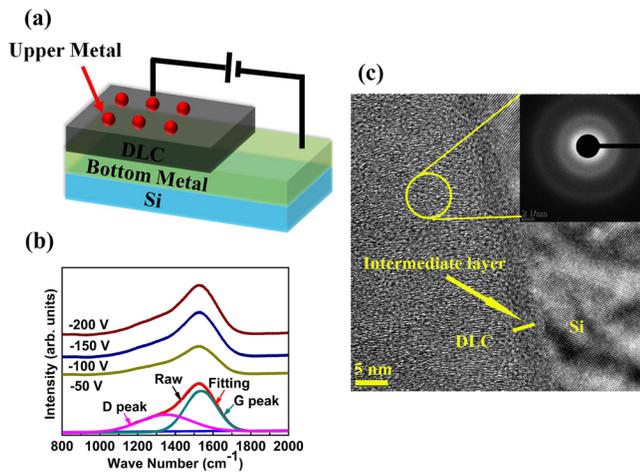
FIG. 1. The schematic diagram of the MSM structure (a), typical Raman spectra of the DLC (b), the cross-sectional HRTEM image, corresponding SAED pattern of the representative DLC deposited at −100 V (c).

adsorbates on the surface, and the cooling rate was kept at about 3 K/min.

Figure 1(b) shows Raman spectra of the DLC films with different bias voltages. All spectra exhibited a broad asymmetric Raman scattering band in the range of 800–2000 cm^{-1}, and no distinct change was visible for the spectra. The fitted data from D and G peaks [G peak position, the intensity ratio of the D-peak to G-peak (I_D/I_G) and the full width at half maximum (FWHM) of the G-peak can be found in the supplementary material] revealed that the carbon atomic bond was similar regardless of bias changes. Figure 1(c) presents the representative cross-sectional high-resolution TEM image and the corresponding selected area electron diffraction (SAED) pattern of the DLC film deposited at −100 V. A dense and diffused diffraction halo was obtained, which implied the typical amorphous structure for DLC films, the H content of the sample at −100 V was also measured by elastic recoil detection analysis (ERD), and $C_{10}O_{0.5}H_{2.6}$ was identified, with H/C + H around 20.6% (supplementary material S1). Besides, XPS confirmed that the O content was less than 1.2 at. % in those deposited films, and $sp^3/sp^2 + sp^3$ was in the range of 44.5%–48.1% (supplementary material).

Figure 2 presents the I-V characteristics of the MSM devices with different contact metal combinations at room temperature. For four MSM devices with the same DLC films, the current intensity varied greatly with different metal contact combinations; at least two factors should be considered for this variance: first, the local inhomogeneity between DLC and metal contact;[9] in addition, the actual film thickness between metal contacts could be quite different since some energetic metal atoms can penetrate deep into the DLC. Noted that as shown in Figs. 2(a)–2(d), all I-V curves of the MSM devices at both positive and negative applied voltages were almost the same in the range of −5 to 5 V, with D_{asy} around 1 [typically shown in Fig. 2(e)]. This highly symmetric current transport process indicated that the DLC/metal interface made slight contribution to the transport process, which could originate from the rich sp^2 regions in the DLC film (more than 50%, as seen in supplementary material, S2) and a large area of upper metal contacts (contact area 3.1×10^{-8} m^2) to DLC.[9,12]

Considering the similar microstructure of the DLC films and the current transport process regardless of the DLC/metal interface, we selected the typical I-V curves of the MSM device with structured Al/DLC(−50 V)/Al to gain insight into the electrical properties and carrier transport mechanism. As shown in Fig. 2(f), in the lower applied voltage range of 0–1 V, the I-V curve exhibited a linear dependence, which indicated the ohmic behavior and could be explained from the hopping conduction at the low electrical field.[11] However, in the higher voltage range of 1–5 V, the I-V curve was well plotted based on the bulk-limited Poole-Frenkel (PF) mechanism as shown in Fig. 2(g).[12,13,15] The I-V relationship could be described as follows:

$$Ln(I/V) \sim V^{1/2}, \tag{1}$$

where I and V are the current and voltage, respectively. Actually, independent of the type and thickness of the contact metal, all I-V curves of the MSM devices with DLC deposited at −50 V matched the PF mechanism well in the voltage range of 1–5 V (as seen in supplementary material
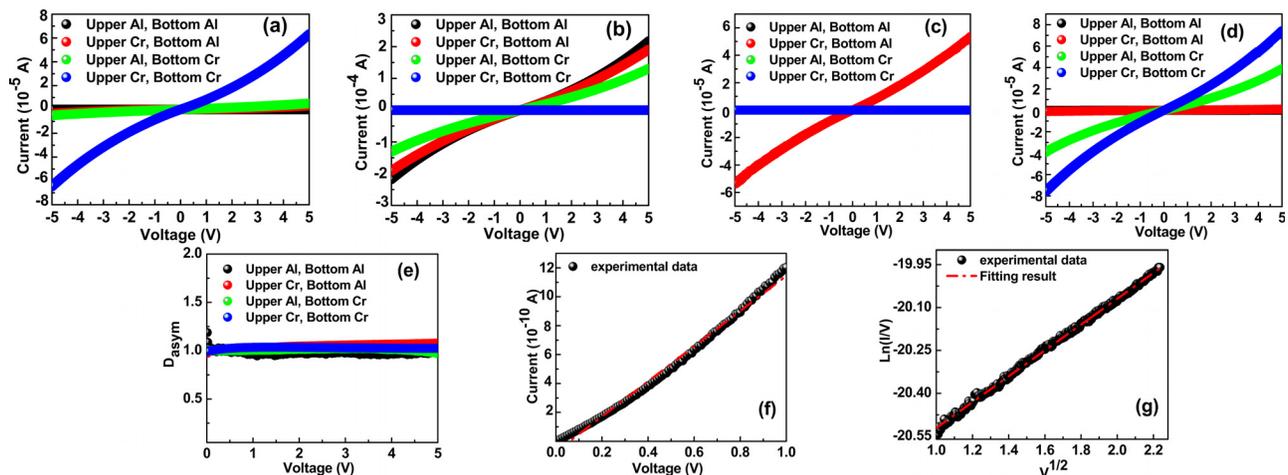
FIG. 2. The I-V curves of MSM structures with DLC deposited at −50 V (a), −100 V (b), −150 V (c) and −200 V (d), the I-V asymmetry of MSM structures with DLC deposited at −50 V (e) and the I-V curves of the MSM device with Al/DLC/Al structure in the range of 0∼1 V (f) and the corresponding Poole-Frenkel plots in the range of 1∼5 V (g).
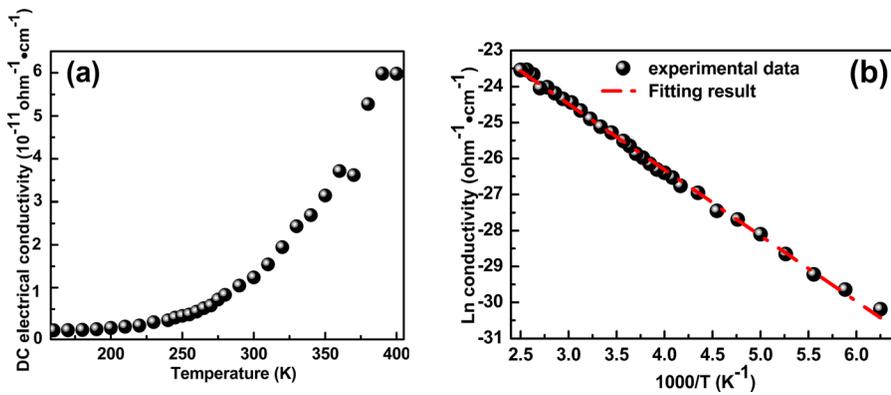
S3), indicating that the current followed the PF mechanism and was limited by thermally assisted hopping at bulk traps in the DLC films.[13,15]

In order to figure out the carrier transport mechanism, the temperature dependence of the dark conductivity (σ) of the MSM device with DLC deposited at -50 V was also studied. As shown in Fig. 3(a), σ increased from the minimum value $7.7 \times 10^{-14} \Omega^{-1}$ cm^{-1} at 160 K to 1.2×10^{-11} Ω^{-1} cm^{-1} at 300 K and reached the maximum value of $6.0 \times 10^{-11} \Omega^{-1}$ cm^{-1} at 400 K, revealing the typical semiconducting behavior of DLC films. Besides, the temperature dependence on the dark conductivity in the range of 160–400 K was consistent with the Arrhenius law,[16–18] with the following σ-T relationship:

$$\sigma(T) = \sigma_0 \exp\left(-\Delta E/(kT)\right), \quad (2)$$

where σ_0 is the pre-exponential index, ΔE is the activation energy, k is the Boltzmann constant, and T is the absolute temperature. The Arrhenius-type σ-T relationship suggested that ΔE was 0.1576 eV, and the carrier transport was dominated by thermally activated process,[15,16] which was also observed in some other weakly conducting carbon films.[13,16,18]

These results can be explained on the basis of the MSM structure and the electric resistance involved. In MSM devices, the contact resistance (R_I) in the metal/semiconductor interface[19,20] and bulk resistance of the semiconductor (R_B) will determine its performances, as shown in Fig. 4, and the I-V should follow a simple relationship

$$V = I(R_{I\,U} + R_B + R_{I\,B}), \quad (3)$$

where $R_{I\,U}$ and $R_{I\,B}$ are the upper metal/DLC contact resistance and the DLC/bottom metal contact resistance, respectively. In this work, the DLC was highly insulated and its RT resistance surpassed the upper limit of a digital multimeter (UNI-T UT39A, 200 MΩ), suggesting a quite large R_B. Then, the situation that R_I is negligible compared with R_B becomes quite possible, and in this case, the electrical behaviors of the MSM devices will mainly depend on R_B since a small voltage drop across the contact resistance and the I-V relationship could be approximately described as $V \approx IR_B$; in other words, the electrical properties of the highly insulated DLC between the metal contacts will determine the bulk-limited and typical semiconducting behaviors of the MSM devices.
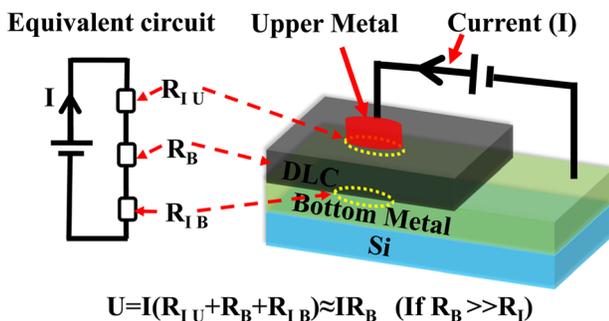
In conclusion, independent of metal combinations, all MSM devices with high-resistance DLC exhibited highly symmetrical I-V behaviors in the range of -5 to 5 V, suggesting bulk-limited electrical properties. For MSM devices with DLC deposited at -50 V, the I-V curves exhibited the ohmic behavior from 0–1 V and followed the Poole-Frenkel mechanism in the range of 1–5 V. Besides, the temperature dependence of the dark conductivity from 160 to 400 K confirmed that the carrier transport was limited by thermally assisted hopping at bulk traps with an activation energy of 0.1576 eV. The bulk-limited and typical semiconducting behaviors of the MSM devices could be explained from the relatively high resistance of bulk DLC.

See supplementary material for the deposition conditions, thickness, O content, sp^3 concentration, the fitted G-peak position, I_D/I_G and FWHM of the G-peak of the DLC, supplementary material S1 for the ERD test of the DLC deposited at -100 V, supplementary material S2 for XPS spectra of the DLC and supplementary material S3 for I-V curves, and corresponding PF plots of the MSM structures for DLC deposited at -50 V.

FIG. 4. Equivalent circuit diagram of the MSM device.

[1]K. Shimakawa and K. Miyake, Phys. Rev. Lett. **61**(8), 994 (1988).
[2]A. Grill, Thin Solid Films **355-356**, 189 (1999).

[3]E. Peiner, A. Tibrewala, R. Bandorf, S. Biehl, H. Lüthje, and L. Doering, Sens. Actuators, A **130-131**, 75 (2006).

[4]Y. C. Jiang and J. Gao, Appl. Phys. Lett. **109**(8), 081104 (2016).

[5]F. Zhuge, W. Dai, C. L. He, A. Y. Wang, Y. W. Liu, M. Li, Y. H. Wu, P. Cui, and R. W. Li, Appl. Phys. Lett. **96**(16), 163505 (2010).

[6]J. L. Xu, D. Xie, C. H. Zhang, X. W. Zhang, P. G. Peng, D. Fu, H. Qian, T. L. Ren, and L. T. Liu, Appl. Phys. Lett. **105**(17), 172101 (2014).

[7]E. Liu, X. Shi, L. K. Cheah, Y. H. Hu, H. S. Tan, J. R. Shi, and B. K. Tay, Solid-State Electron. **43**, 427 (1999).

[8]M. Allon-Alaluf, L. Klibanov, A. Seidman, and N. Croitoru, Diamond Relat. Mater. **5**, 1275 (1996).

[9]S. Paul and F. J. Clough, Appl. Phys. Lett. **78**, 1415 (2001).

[10]A. P. Zeng, Y. B. Yin, M. Bilek, and D. McKenzie, Surf. Coat. Technol. **198**(1-3), 202 (2005).

[11]F. M. Wang, M. W. Chen, and Q. B. Lai, Thin Solid Films **518**(12), 3332 (2010).

[12]S. Paul and F. J. Clough, Diamond Relat. Mater. **7**, 1734 (1998).

[13]S. Egret, J. Robertson, W. I. Milne, and F. J. Clough, Diamond Relat. Mater. **6**, 879 (1997).

[14]W. Dai, H. Zheng, G. S. Wu, and A. Y. Wang, Vacuum **85**(2), 231 (2010).

[15]C. Godet, S. Kumar, and V. Chu, Philos. Mag. **83**(29), 3351 (2003).

[16]S. Bhattacharyya and S. R. P. Silva, Thin Solid Films **482**(1-2), 94 (2005).

[17]E. Staryga and G. W. Bak, Diamond Relat. Mater. **14**, 23 (2005).

[18]M. Koós, S. H. S. Moustafa, E. Szilágyi, and I. Pócsik, Diamond Relat. Mater. **8**, 1919 (1999).

[19]R. T. Tung, Appl. Phys. Rev. **1**(1), 011304 (2014).

[20]L. J. Brillson and Y. C. Lu, J. Appl. Phys. **109**(12), 121301 (2011).